Stabilizing Inverted Pendulum using Pontryagin Minimal Principle based Quadratic Controller and H_∞ Loop Controller *

*Note: Sub-titles are not captured in Xplore and should not be used

Labid Bin Bashar
23822701
labid.bashar@gmail.com

Abdul Hamid
23822002
hamidabdul776@outlook.co.id

***Abstract*—The control of an inverted pendulum on a cart (IPOC) system is a challenging problem in control systems research due to its inherent instability and complex dynamics. This paper investigates various optimal control techniques and robust control strategies for addressing the control problem of the IPOC system. The Pontryagin's Minimum Principle (PMP) is employed as a mathematical framework for determining the optimal control policy. Linear Quadratic Control (LQC). Robust control techniques, particularly the H-infinity loop shaping control, are explored for ensuring system stability and performance in the presence of uncertainties and disturbances. Simulation results demonstrate the effectiveness of the proposed controllers in stabilizing the IPOC system, with optimal controllers minimizing a cost function associated with the system's performance. The H-infinity loop controller exhibits robustness against uncertainties and disturbances, providing superior disturbance rejection compared to the LQR controller. The study concludes by highlighting the advantages and limitations of each control technique and emphasizes the importance of selecting the appropriate control strategy based on specific system requirements and constraints. The findings contribute to the advancement of control theory and provide valuable insights for addressing complex control problems in various applications.**

***Index Terms*—LQR, H_∞ Loop Controller, Loop Shaping, Linear Fractional Transformation, Riccati Equation**

I. Introduction

The control of an inverted pendulum mounted on a cart (IPOC) [1], [2] has emerged as a captivating research topic within the field of control theory. The inherent instability and complex dynamics of the inverted pendulum system on a cart make it an intriguing subject for investigation. This study aims to explore the underlying reasons that motivate the control of an inverted pendulum in a cart, addressing the significance of this problem in the context of control systems research. By examining this challenging system, valuable insights can be gained regarding the fundamental principles of stability, control methodologies, and the development of robust control strategies. Understanding the control of the inverted pendulum in a cart contributes to the advancement of control theory and provides a foundation for tackling intricate control problems in diverse applications.Numerous techniques have been investigated with a view to solving the inverted pendulum control problem. Optimal control techniques have emerged as powerful tools for achieving desired performance and stability in control systems. By formulating the control problem as an optimization task, optimal controllers aim to minimize a specific cost function while meeting system constraints. In addition to optimality, robustness is another crucial aspect of control system design. Real-world systems are often subject to uncertainties, disturbances, and variations in operating conditions. Robust control techniques address these challenges by aiming to ensure system stability and performance despite uncertainties.

Over the years, significant advancements have been made in the development and application of optimal controllers as well as robust controller in various fields. One of the earliest and most well-known optimal control techniques is the Pontryagin's Minimum Principle (PMP) [3]. PMP provides a powerful mathematical framework for determining the optimal control policy for a given system. By formulating the control problem as an optimization problem and incorporating the system dynamics and cost function, PMP yields necessary conditions that the optimal control must satisfy. This principle has been widely used in diverse applications, ranging from aerospace systems to robotics. PMP can be employed to design Linear Quadratic control (LQC) [4]. LQC is based on a state-space model of the system and involves minimizing a quadratic cost function. By solving the associated Riccati equation, the optimal control gains can be obtained. LQC has been extensively applied in various domains, including aerospace [5], robotics [6], and process control [7]. Another widely used optimal control technique is Linear Quadratic Gaussian (LQG) control [8]. LQG combines the optimal control of LQC with the estimation of system states using a Kalman filter. By incorporating state estimation, LQG control is capable of handling noisy measurements and uncertainties in the system dynamics. Model Predictive Control (MPC) [9] is a popular optimal control strategy that has gained significant attention in recent years. MPC is a receding horizon control approach that

Identify applicable funding agency here. If none, delete this.

solves a finite-horizon optimization problem at each sampling instant. By considering system dynamics, constraints, and a cost function, MPC computes an optimal control sequence over the prediction horizon. The first control action is then applied to the system, and the optimization process is repeated at the next sampling instant. In the field of robust control design, one prominent technique in robust control is the H-infinity [10] loop shaping control, often referred to as the H-loop controller. The H-infinity control framework aims to optimize the closed-loop performance while guaranteeing robustness against uncertainties and disturbances. The H-loop controller offers several advantages. Firstly, it provides a systematic approach to address uncertainties in the system. By considering a weighted H-infinity norm as the performance measure, the controller design process incorporates robustness requirements. This allows the controller to maintain satisfactory performance even in the presence of modeling errors, external disturbances, and parameter variations. Secondly, the H-loop controller can handle both continuous-time and discrete-time systems, making it applicable to a wide range of control problems. Additionally, it supports the inclusion of constraints, such as input and output bounds, to ensure the practical feasibility of the control actions [11].

Despite the advantages of optimal as well as robust controller, in many cases one or both of them fails to satisfy the requirements of the designer in stability, performance or efficiency. That's why, this paper contributes to the design of the Pontryagin Minimal Principle based Quadratic Controller and the H_∞ loop controller separately for stabilizing the inverted pendulum on a cart. After comparing the stability, performance and efficiency criteria, it will be shown that one technique is superior to another under some specified conditions. The composition of the can be arranged as follows: In the Section II, the technique of designing the controllers for inverted pendulum and curved have been described. In the section III, the results from the system have been given and analyzed with comparison. The paper has been concluded making a remark in the conclusion section IV.

II. System Modelling

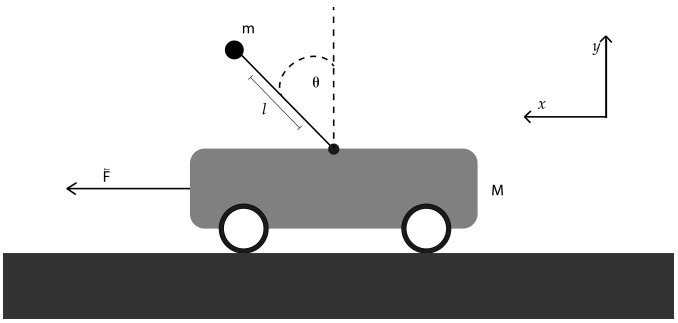

Fig. 1. Inverted Pendulum on a Cart

Figure 1 illustrates the dynamics of any inverted pendulum on a cart according to [12]. If x be the cart position at any instant, v is the velocity, θ is the pendulum angle, ω is the angular velocity, m is the pendulum mass, M is the cart mass, L is the pendulum arm, g is the gravitational acceleration, b is a friction coefficient on the cart, and F is a force applied to the cart, the dynamics of the system can be derived either by Newton's law or Lagrangian method. Clearly, the state vector of the system is $q = \begin{bmatrix} x & v & \theta & \omega \end{bmatrix}^\intercal$ and control variable is $u = F$. Now changing the notation of the states to new notation we get, $q = \begin{bmatrix} x_1 & x_2 & x_3 & x_4 \end{bmatrix}^\intercal$. Now, system of equations for IPOC can be given by,

$$\dot{x}_1 = f_1 = x_2 \tag{1}$$

$$\dot{x}_2 = f_2 = \frac{(-m^2L^2g\cos x_3 \sin x_3}{mL^2(M + m(1 - \cos {x_3}^2)} + \frac{mL^2(mLx_4^2 \sin x_3 - bx_2) + mL^2u}{mL^2(M + m(1 - \cos {x_3}^2)} \tag{2}$$

$$\dot{x}_3 = f_3 = x_4 \tag{3}$$

$$\dot{x}_4 = f_4 = \frac{(m + M)mgL \sin x_3}{mL^2(M + m(1 - \cos {x_3}^2))} + \frac{-mL\cos x_3(mLx_4^2 \sin x_3 - bx_2) + mL\cos x_3 u}{mL^2(M + m(1 - \cos {x_3}^2))}. \tag{4}$$

Here, (1)-(4) are nonlinear equations. In general, they are expressed as $\dot{(q)} = f(q, u)$. Now doing first order Taylor's expansion on the equation around a specified equilibrium point (q^*, u^*) we get,

$$f(q,u) \approx f(q^*,u^*) + \left.\frac{\partial f(q,u)}{\partial q}\right|_{q=q^*} (q - q^*) + \left.\frac{\partial f(q,u)}{\partial u}\right|_{u=u^*} (u - u^*). \tag{5}$$

Clearly, $\frac{\partial f(q,u)}{\partial q}$ and $\frac{\partial f(q,u)}{\partial u}$ are Jacobian matrices. Around (q^*, u^*), these matrices are nothing but approximated as system matrix A and input matrix B. Therefore, (5) can be rewritten as,

$$f(q,u) \approx f(q^*,u^*) + A(q - q^*) + B(u - u^*). \tag{6}$$

Now we will make two assumptions. First, at equilibrium point, the system dynamics is static and does not change over time anymore. So, we get, $f(q^*, u^*) = 0$. Again, for all instance in time horizon, the system works at the neighbourhood of the equilibrium points. Hence, under these assumptions, The state space equation thus is written as,

$$\dot{q} \approx Aq + Bu. \tag{7}$$

Again, let the output matrix be $C = \begin{bmatrix} 1 & 0 & 0 & 0 \end{bmatrix}$. As sensor is not mounted at the same spot u is acted on, system input does not directly influence the system output. Hence $D = 0$.

Therefore, if the pendulum needs to be stabilized upright $x_3 = \pi$, the IPOC system can be modelled as,

$$\dot{q} = \begin{bmatrix} \dot{x}_1 \\ \dot{x}_2 \\ \dot{x}_3 \\ \dot{x}_4 \end{bmatrix} = \begin{bmatrix} 0 & 1 & 0 & 0 \\ 0 & -\frac{b}{M} & \frac{mg}{M} & 0 \\ 0 & 0 & 0 & 1 \\ 0 & -\frac{b}{ML} & -\frac{(M+m)g}{ML} & 0 \end{bmatrix} \begin{bmatrix} x_1 \\ x_2 \\ x_3 \\ x_4 \end{bmatrix} + \begin{bmatrix} 0 \\ \frac{1}{M} \\ 0 \\ \frac{1}{ML} \end{bmatrix} u \quad (8)$$

$$y = \begin{bmatrix} 1 & 0 & 0 & 0 \end{bmatrix} \begin{bmatrix} x_1 \\ x_2 \\ x_3 \\ x_4 \end{bmatrix} + Du \quad (9)$$

Thus, (8)-(9) model the IPOC as a Linear time-invariant system around the equilibrium point.

III. Optimal Controller Design

Consider that, at every time step, measurement information all the states are available. Based on the system model the objective of an optimal controller is to ensure stability of the system optimizing a cost function over a finite or infinite time. Stabilizing the configuration of IPOC is finite horizon problem because, In this case, the control problem is formulated with a specific goal of stabilizing the pendulum within a finite duration. The control inputs are designed to bring the system into a stable configuration and maintain it over the given time interval. The cost function is designed to penalize deviations from the desired state. Here, the deviation at any time t is $e(t) = q_g(t) - Cq(t)$; $q_g = \begin{bmatrix} x_{1,g} & x_{2,g} & x_{3,g} & x_{4,g} \end{bmatrix}^\intercal$ being the final configuration of IPOC to be stabilized before time t_f. In this regard, the error vector and cost function can be given by,

$$e(t) = \begin{bmatrix} e_1(t) \\ e_2(t) \\ e_3(t) \\ e_4(t) \end{bmatrix} = \begin{bmatrix} x_{1,g} \\ x_{2,g} \\ x_{3,g} \\ x_{4,g} \end{bmatrix} - C \begin{bmatrix} x_1(t) \\ x_2(t) \\ x_3(t) \\ x_4(t) \end{bmatrix} \quad (10)$$

$$J = \frac{1}{2} e(t_f)^\intercal F(t_f) e(t_f) + \frac{1}{2} \int_{t_0}^{t_f} e(t)^\intercal Q e(t) + u^\intercal R u \, dt, \quad (11)$$

where $F(t_f)$ is the terminal cost matrix, Q is the error weighted matrix and R is the control weighted matrix. If Q and R are constant matrices, the cost function becomes,

$$J = \frac{1}{2} \int_{t_0}^{t_f} \Bigg(\begin{bmatrix} e_1(t) & e_2(t) & e_3(t) & e_4(t) \end{bmatrix} \begin{bmatrix} \kappa_1 & 0 & 0 & 0 \\ 0 & \kappa_2 & 0 & 0 \\ 0 & 0 & \kappa_3 & 0 \\ 0 & 0 & 0 & \kappa_4 \end{bmatrix} \begin{bmatrix} e_1(t) \\ e_2(t) \\ e_3(t) \\ e_4(t) \end{bmatrix} + u^\intercal \begin{bmatrix} r \end{bmatrix} u \Bigg) dt, \quad (12)$$

Now, let us define the Hamiltonian as,

$$H = \frac{1}{2} \begin{bmatrix} e_1(t) & e_2(t) & e_3(t) & e_4(t) \end{bmatrix} \begin{bmatrix} \kappa_1 & 0 & 0 & 0 \\ 0 & \kappa_2 & 0 & 0 \\ 0 & 0 & \kappa_3 & 0 \\ 0 & 0 & 0 & \kappa_4 \end{bmatrix} \begin{bmatrix} e_1(t) \\ e_2(t) \\ e_3(t) \\ e_4(t) \end{bmatrix} + \frac{1}{2} r u^2 + \begin{bmatrix} \lambda_1 & \lambda_2 & \lambda_3 & \lambda_4 \end{bmatrix} \Bigg(\begin{bmatrix} 0 & 1 & 0 & 0 \\ 0 & -\frac{b}{M} & \frac{mg}{M} & 0 \\ 0 & 0 & 0 & 1 \\ 0 & -\frac{b}{ML} & -\frac{(M+m)g}{ML} & 0 \end{bmatrix} \begin{bmatrix} x_1 \\ x_2 \\ x_3 \\ x_4 \end{bmatrix} + \begin{bmatrix} 0 \\ \frac{1}{M} \\ 0 \\ \frac{1}{ML} \end{bmatrix} u \Bigg), \quad (13)$$

where, $\lambda = \begin{bmatrix} \lambda_1 & \lambda_2 & \lambda_3 & \lambda_4 \end{bmatrix}^\intercal$ is the co-state vector. Equation (13) can be further broken down into following equation,

$$H = \frac{1}{2}(\kappa_1 e_1^2 + \kappa_2 e_2^2 + \kappa_3 e_3^2 + \kappa_4 e_4^2) + \frac{1}{2} r u^2 + \lambda_1 x_1 - \lambda_2 \left(\frac{b x_2 - mg x_3}{M}\right) + \lambda_3 x_4 - \lambda_4 \left(\frac{b x_2 + (M+m) g x_3}{ML}\right) + \left(\frac{\lambda_2}{M} + \frac{\lambda_4}{ML}\right) u. \quad (14)$$

Now, taking the partial derivative of H with respect to u and set it zero we get the open loop optimal control as follows,

$$\frac{\partial H}{\partial u} = 0, \quad \implies r u^* + \begin{bmatrix} 0 & \frac{1}{M} & 0 & \frac{1}{ML} \end{bmatrix} \lambda^* = 0 \quad (15)$$

$$\implies u^* = -\frac{1}{r} \begin{bmatrix} 0 & \frac{1}{M} & 0 & \frac{1}{ML} \end{bmatrix} \begin{bmatrix} \lambda_1 \\ \lambda_2 \\ \lambda_3 \\ \lambda_4 \end{bmatrix}_{\lambda = \lambda^*} \quad (16)$$

$$\implies u^* = -\frac{1}{rML} (\lambda_2^* L + \lambda_4^*). \quad (17)$$

It is evident that, the open loop optimal control law $u*$ directly depends on the optimal costates λ_2^* and λ_4^*. Hence it is required to determine the optimal costates which further requires Hamiltonian canonical system to be determined. so, the system can be given by the following equation,

$$\dot{q} = \frac{\partial H}{\partial \lambda} \quad (18)$$

$$\dot{\lambda} = -\frac{\partial H}{\partial q}. \quad (19)$$

Now putting the values of (13) and (16) or (17) in the equation (18) we get,

$$\dot{q}^* = \begin{bmatrix} \dot{x}_1 \\ \dot{x}_2 \\ \dot{x}_3 \\ \dot{x}_4 \end{bmatrix}_{q=q^*} = \begin{bmatrix} 0 & 1 & 0 & 0 \\ 0 & -\frac{b}{M} & \frac{mg}{M} & 0 \\ 0 & 0 & 0 & 1 \\ 0 & -\frac{b}{ML} & -\frac{(M+m)g}{ML} & 0 \end{bmatrix} \begin{bmatrix} x_1 \\ x_2 \\ x_3 \\ x_4 \end{bmatrix}_{q=q^*} - \frac{1}{r} \begin{bmatrix} 0 \\ \frac{1}{M} \\ 0 \\ \frac{1}{ML} \end{bmatrix} \begin{bmatrix} 0 & \frac{1}{M} & 0 & \frac{1}{ML} \end{bmatrix} \begin{bmatrix} \lambda_1 \\ \lambda_2 \\ \lambda_3 \\ \lambda_4 \end{bmatrix}_{\lambda = \lambda^*} \quad (20)$$

Again, from the (19) the following equation is obtained,

$$\dot{\lambda}^* = \begin{bmatrix} \dot{\lambda}_1 \\ \dot{\lambda}_2 \\ \dot{\lambda}_3 \\ \dot{\lambda}_4 \end{bmatrix}_{\lambda=\lambda^*} = \begin{bmatrix} \kappa_1 & 0 & 0 & 0 \\ 0 & \kappa_2 & 0 & 0 \\ 0 & 0 & \kappa_3 & 0 \\ 0 & 0 & 0 & \kappa_4 \end{bmatrix} \begin{bmatrix} x_1 \\ x_2 \\ x_3 \\ x_4 \end{bmatrix}_{q=q^*} - \begin{bmatrix} 0 & 0 & 0 & 0 \\ 1 & -\frac{b}{M} & 0 & -\frac{b}{ML} \\ 0 & \frac{mg}{M} & 0 & -\frac{(m+M)g}{ML} \\ 0 & 0 & 1 & 0 \end{bmatrix} \begin{bmatrix} \lambda_1 \\ \lambda_2 \\ \lambda_3 \\ \lambda_4 \end{bmatrix}_{\lambda=\lambda^*} + \begin{bmatrix} \kappa_1 & 0 & 0 & 0 \\ 0 & \kappa_2 & 0 & 0 \\ 0 & 0 & \kappa_3 & 0 \\ 0 & 0 & 0 & \kappa_4 \end{bmatrix} \begin{bmatrix} x_{1,g} \\ x_{2,g} \\ x_{3,g} \\ x_{4,g} \end{bmatrix} \quad (21)$$

It is to be noted that, (20)-(21) express the full Hamiltonian canonical system. Being 8 dimensional system, the equations are repacked in matrix format as follows,

$$\begin{bmatrix} \dot{q}^* \\ \dot{\lambda}^* \end{bmatrix} = \begin{bmatrix} A & -Br^{-1}B^\intercal \\ -Q & A^\intercal \end{bmatrix} \begin{bmatrix} q^* \\ \lambda^* \end{bmatrix} + \begin{bmatrix} 0 \\ Q \end{bmatrix} q_g \quad (22)$$

Putting the values of boundary conditions the costate vector at terminal time,

$$\lambda(t_f) = F(t_f)(q(t_f) - q_q), \quad (23)$$

showing that state and costates pose a linear relationship between them as,

$$\lambda^*(t) = P(t)(q^*(t) - q_g), \quad (24)$$

where $P(t)$ should be yet determined to satisfy Hamiltonian system (22). Differentiating (24) with respect to time and substituting the λ^* and q^* the following equation will be obtained as,

$$(\dot{P}(t) + P(t)A + A^\intercal P(t) - \frac{P(t)BB^\intercal P(t)}{r} + Q)(q_g - q^*(t)) = 0 \quad (25)$$

from which the matrix Differential Riccati Equation can be given by,

$$\dot{P}(t) + P(t)A + A^\intercal P(t) - \frac{P(t)BB^\intercal P(t)}{r} + Q = 0 \quad (26)$$

The solution of (26) is then employed in (16) to obtain the closed loop optimal control as,

$$u^* = -\frac{1}{r}\begin{bmatrix} 0 & \frac{1}{M} & 0 & \frac{1}{ML} \end{bmatrix} \begin{bmatrix} p_{11}(t) & p_{12}(t) & p_{13}(t) & p_{14}(t) \\ p_{21}(t) & p_{22}(t) & p_{23}(t) & p_{24}(t) \\ p_{31}(t) & p_{32}(t) & p_{33}(t) & p_{34}(t) \\ p_{41}(t) & p_{42}(t) & p_{43}(t) & p_{44}(t) \end{bmatrix} \begin{bmatrix} e_1(t) \\ e_2(t) \\ e_3(t) \\ e_4(t) \end{bmatrix}, \quad (27)$$

where $P(t)$ has been expressed in matrix form. Thus (27) represents the Linear Quadratic controller derived using Pontryagin Minimal Principle.

IV. H_∞ Loop Controller

In the previous section, it has been shown how Optimal Controller has been obtained using DRE (26). In Usually optimal controller cannot ensure enough margin to the system. Therefore, in presence of disturbances and uncertainty, the possibility that the system could approach to instability cannot be ignored. Therefore, H_∞ Loop controller, a robust approach can be employed to ensure the robustness of the closed loop system despite having uncertainty and disturbance. Hence, the obtaining an linear controller

$$u = Kq, \quad (28)$$

in such a way that the finite(or infinite) horizon ∞-norm of the closed loop system

$$||S_{zw}||_\infty < \gamma, \quad (29)$$

mapping w to z is less than some value γ. the parameter γ represents the desired performance level or tolerance for the closed-loop system. It is a user-defined value that specifies the maximum allowable sensitivity of the regulated output z to exogenous input w. Hence, introducing uncertainty to the IPOC (8) in form of e w, the augmented system equation is,

$$\begin{bmatrix} \dot{q} \\ z \\ y \end{bmatrix} = \begin{bmatrix} A & B_1 & B_2 \\ C_1 & D_{11} & D_{12} \\ C_2 & D_{21} & D_{22} \end{bmatrix} \begin{bmatrix} q \\ w \\ u \end{bmatrix}, \quad (30)$$

where the objective signal can be given by,

$$z = C_1 q + D_{11} w D_{12} u, \quad (31)$$

A is a 4×4 matrix, B_1 is a $4 \times m$ matrix where represents the number of exogenous input to the system. B_2 is same as B in the optimal controller being 4×1 vector. The dimensions of C_1, C_2, D_{12} and D_{21} are respectively $q \times 4$, 1×4, $q \times 1$, $1 \times m$, where q denotes the the number of elements in the regulated output z. Finally, both D_{11} and D_{22} are $\begin{bmatrix} 0 \end{bmatrix}$ with corresponding dimensions being $q \times m$ and 1×1. Let us assume that (A, B_1) is stabilizable, meaning that there exists a state-feedback control law that can stabilize the system. Additionally, the pair (C_1, A) is detectable, indicating that it is possible to design an observer that can accurately estimate the system's unmeasured states based on the available measurements. Moreover, the pair (A, B_2) is stabilizable, implying that there exists another state-feedback control law that can stabilize a different aspect of the system. Lastly, the pair (C_2, A) is detectable, indicating the possibility of designing an observer to estimate the unmeasured states related to this aspect of the system.

A. Controller Synthesis Using Single Riccati

Let us first consider the problem as a regulator problem for the simplicity of synthesis. In this case, m and q are 2 because of two exogenous inputs and two regulated outputs, z_1 and z_2. In this case, w_1 can be regarded as model uncertainty due to

external or internal disturbance, whereas w_2 is sensor noise. Hence, (32) is transformed to

$$\begin{bmatrix} \dot{q} \\ z \\ y \end{bmatrix} = \begin{bmatrix} A & B_1 & B_2 \\ C_1 & 0 & D_{12} \\ C_2 & D_{21} & 0 \end{bmatrix} \begin{bmatrix} q \\ w \\ u \end{bmatrix}, \tag{32}$$

where both $D_{12}^\intercal D_{12}$ and $D_{21}^\intercal D_{21}$ are identity matrices I. The objective signal (31) thus converted to,

$$z = C_1 q + D_{12} u. \tag{33}$$

The new objective signal (33) indicates that, $z^\intercal z$ has cross terms between u and q that eventually complicate the future analyses using this formula of $z^\intercal z$. Therefore, the standard augmentation can be brought in the (32) as follows,

$$\dot{q} = A_a q + B_1 w + B_{2,a} u \tag{34}$$

$$z = \begin{bmatrix} C_a q & D_a u \end{bmatrix}^\intercal \tag{35}$$

$$y = C_2 q + D_{21} w, \tag{36}$$

where A_a, $B_{2,a}$, C_a and D_a can be given by,

$$A_a = A - B_2 D_{12}^\intercal C_1 \tag{37}$$

$$B_{2,a} = D_{12}^\intercal C_1 q \tag{38}$$

$$C_a^\intercal C_a = C_1^\intercal (I - D_{12} D_{12}^\intercal) C_1 \tag{39}$$

$$D_a = D_{12}^\intercal C_1 q. \tag{40}$$

With a view to holding the condition to designing the H_∞ loop controller with a finite time Horizon T (from t_0 to t_f), the following condition should be satisfied:

$$\int_{t_0}^{t_f} (z^\intercal z - \gamma^2 w^\intercal w) dt + q^\intercal(t_f) \Delta q(t_f) \leq -\epsilon ||w||^2_{2,[t_0, t_f]}, \tag{41}$$

where $epsilon > 0$ and Δ is non-negative matrix.Now with similar process as in the optimal controller section, the Hamiltonian system can be given by,

$$\begin{bmatrix} \dot{q} \\ \dot{\lambda} \end{bmatrix} = \begin{bmatrix} A_a & -(B_{2,a} B_{2,a}^\intercal - \gamma^2 B_1 B_1^\intercal) \\ -C_a^\intercal C & -A_a^\intercal \end{bmatrix} \begin{bmatrix} q \\ \lambda \end{bmatrix} \tag{42}$$

Putting the boundary conditions and using the (42) the DRE becomes,

$$\dot{P}(t) + P(t) A_a + A_a^\intercal P(t) - P(t)(B_{2,a} B_{2,a}^\intercal - \gamma^2 B_1 B_1^\intercal) P(t) + C_a^\intercal C_a = 0 \tag{43}$$

The solution of DRE (43) is used to obtain the H_∞ loop controller in the following way,

$$u = -B_{2,a} P(t) \tag{44}$$

This is how the H_∞ for the IPOC system can be synthesized. It is to be noted that, $B_{2,a}$ is a 4×4 matrix.

B. Controller Synthesis Using Double DRE

Considering the (32), for IPOC, it can be shown that, $D_{12}^\intercal \begin{bmatrix} C_1 & D_{12} \end{bmatrix} = \begin{bmatrix} 0 & I \end{bmatrix}$ and $\begin{bmatrix} B_1 & D_{21} \end{bmatrix}^\intercal D_{21}^\intercal = \begin{bmatrix} 0 & I \end{bmatrix}^\intercal$. If two DREs can be given by,

$$\dot{P}(t) + P(t) A + A^\intercal P(t) - P(t)(B_1 B_1^\intercal / \gamma^2 - B_2 B_2^\intercal) P(t) + C_1^\intercal C_1 = 0 \tag{45}$$

$$\dot{N}(t) + N(t) A^\intercal + A N(t) - N(t)(C_1^\intercal C_1 / \gamma^2 - C_2^\intercal C_2) N(t) B_1 B_1^\intercal = 0, \tag{46}$$

and if $P(t)$ and $N(t)$ are ≥ 0, the maximum eigenvalue of $P(t)N(t)$ is $\leq \gamma^2$, then (29) exists and the suboptimal H_∞ loop controller can be given by

$$K_{Ric,2} = \begin{bmatrix} k_{11} & k_{12} \\ k_{21} & 0 \end{bmatrix}, \tag{47}$$

where,

$$k_{11} = A + \gamma^{-2} B_1 B_1^\intercal P(t) + B_2 k_{21} - k_{12} C_2$$

$$k_{12} = -(I - \gamma^{-2} N(t) P(t))^{-1} N(t) C_2^\intercal$$

$$k_{21} = -B_2^\intercal P(t)$$

Thus, $K_{Ric,2}$ is the the controller that can be designed to solve two DRE (45)-(46).

C. Linear Fractional Transformation and Loop Shaping

Till now, the H_∞ controller has been synthesized by the state-space approach. Now (32) can be written in

$$\begin{bmatrix} z \\ y \end{bmatrix} = G(s) \begin{bmatrix} w \\ u \end{bmatrix}, \tag{48}$$

transfer function form where,

$$G(s) = \begin{bmatrix} G_{11}(s) & G_{12}(s) \\ G_{21}(s) & G_{22}(s) \end{bmatrix} = \begin{bmatrix} 0 & D_{12} \\ D_{21} & 0 \end{bmatrix} + \begin{bmatrix} C_1 \\ C_2 \end{bmatrix} (sI - A) \begin{bmatrix} B_1 & B_2 \end{bmatrix}. \tag{49}$$

Therefore, the closed loop system S_{zw} can be written in form of Linear Fractional Transformation (LFT) as

$$S_{zw} = \underline{S}(G, K) = G_{11} + G_{12} K (I - G_{22} K)^{-1} G_{21}, \tag{50}$$

where, K is the control gain that has already mention in (28). The suboptimal controller with internal stabilizing gain

$$K = \begin{bmatrix} A_k & B_k \\ C_k & D_k \end{bmatrix} \tag{51}$$

can be obtained using the condition (29) in LFT as

$$||\underline{S}(G, K)||_\infty \leq \gamma. \tag{52}$$

If the perturbation weight matrix can be given by Δ the LFT will be given by,

$$\bar{S}(G, \Delta) = G_{22} + G_{21} \Delta (I - G_{11} \Delta)^{-1} G_{12}, \tag{53}$$

where Δ can be given by,

$$\Delta = \begin{bmatrix} \delta_1 & 0 \\ 0 & \delta_2 \end{bmatrix}, \tag{54}$$

δ_1 and δ_2 are weighting term for w_1 and w_2 respectively. The whole regulator system is given by the interconnection of two LFTs in fig. (draw a figure of lft as in green 4.7). The H_∞ loop controller can also be designed using loop-shaping technique. The systematic procedure for designing a loop-shaping controller in H_∞ control involves several steps. First, scaling the plant's inputs and outputs improves problem conditioning and simplifies weight selection. Next, ordering the inputs and outputs to diagonalize the plant facilitates the design of diagonal pre- and post-compensators. These compensators shape the system's singular values, with desired characteristics such as high gain at low frequencies and appropriate roll-off rates. Additional weights can be used for singular value alignment and actuator control. Robust stabilization is achieved by calculating the stability margin and synthesizing a suboptimal controller. Analysis and modification ensure that design specifications are met. Finally, the designed controller is implemented in the control system. This systematic procedure ensures performance requirements and robustness in the presence of uncertainties and disturbances.

V. Results and Discussion

The IPOC system parameters can be given by the the I. Therefore the system matrix and the input matrix can be given

TABLE I
System Parameter of IPOC

Parameter	Values
m	1 Kg
M	5 Kg
L	2 m
g	9.8 m/s^2
d	1

by,

$$A = \begin{bmatrix} 0 & 1 & 0 & 0 \\ 0 & -0.2 & 2 & 0 \\ 0 & 0 & 0 & 1 \\ 0 & -0.1 & -6.0 & 0 \end{bmatrix}, \quad B = \begin{bmatrix} 0 & 0.2 & 0 & 0.1 \end{bmatrix}^\intercal$$

A. Optimal Controller

From the Theory with equation(25) we provided system dynamics, state equations, and controller design. We used numerical integration techniques, such as the "ode45" function, to solve the system's ordinary differential equations. and we put all of the variables mentioned in Table(1) as the system parameter of IPOC. We run the simulation involving specif the initial conditions for the state variables and reference position, defining the control law, and integrating the system equations over a desired time span. and to simulate the optimal controller we use the Linear Quadratic Regulator (LQR) approach. The LQR controller design involved formulating a cost function that captures the system's performance objectives. The cost function consisted of quadratic terms for the state variables and control input, and weighting matrices was chosen to balance the trade-off between control effort and state tracking. The optimal control gain was computed by solving the algebraic Riccati equation.

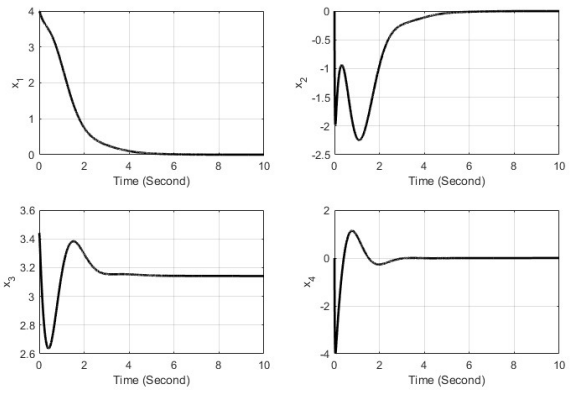

Fig. 2. State Variables

Figure 2 shows the evolution of the state variables over time. The plots depict the position (x_1), velocity (x_2), angle (x_3), and angular velocity (x_4) of the system. Hence, the system is stable.

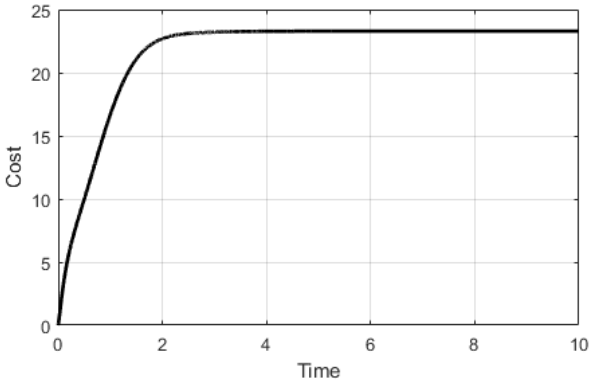

Fig. 3. cost function

from figure 3 we get the result if the cost function on this system has a value 24 in 2 seconds. that mean indicates the overall performance of the controlled system. Lower cost values represent better control performance. The cost stabilizing after around 2 seconds suggests a stable state where control actions effectively maintain the desired position. Overall, the LQR controller successfully achieves stable and satisfactory performance, reflected by the low-cost value and system stabilization. Optimal control systems can be implemented through dynamic programming, using an approach that breaks down complex problems into smaller subproblems. The steps involve building a dynamic model of the system, formulating a value function that reflects the control objective, using the Bellman equation to connect the current state's value function to the future, and developing an iterative algorithm to search for the optimal solution. Dynamic programming enables us to efficiently find the optimal control policy for the system. And

for that equation (2), we have derived a nonlinear equation by using the Taylor expansion of the Jacobian matrix, resulting in the final equation as shown in equation (6).

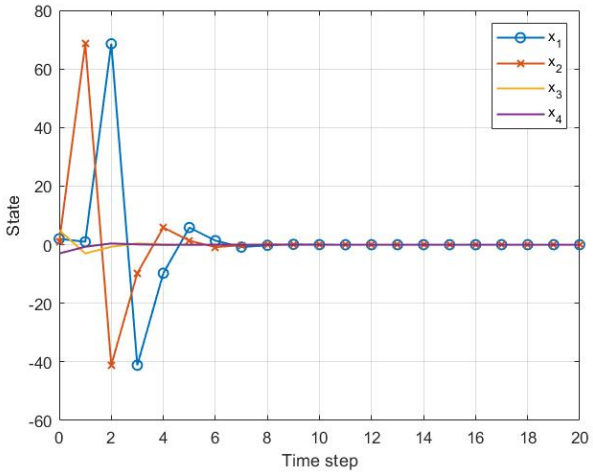

Fig. 4. LQR by dyanmic programming: States

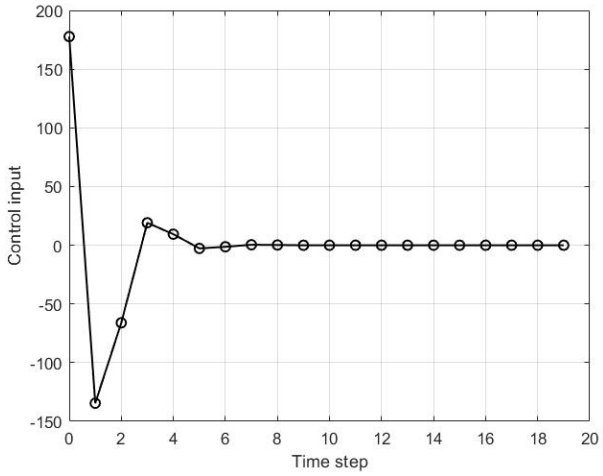

Fig. 5. LQR by dyanmic programming: Control

After we derive the differential Riccati equation by considering the time derivative of the algebraic Riccati equation (45). This equation involves the system dynamics, cost function, and the derivative of the value function. Solve the differential Riccati equation numerically or analytically to obtain the time-varying optimal control gain. Implement this gain in the control law to compute the control input that minimizes the cost function over time.

B. H_∞ Loop Controller

We added extra input and output matrices, denoted as B1 and C1, respectively. This augmentation was done to account for additional control objectives or constraints that were not originally captured by the base system dynamics. The reason

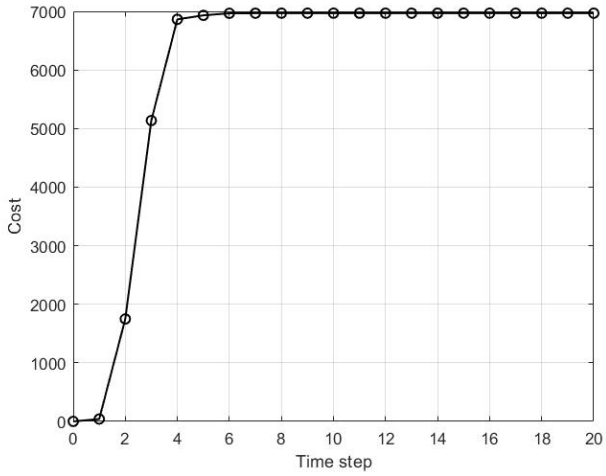

Fig. 6. LQR by dyanmic programming: Cost Function

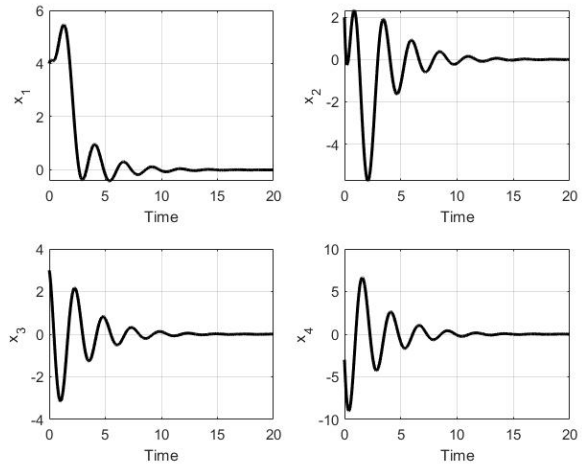

Fig. 7. LQR by Solving DRE by Euler method: States

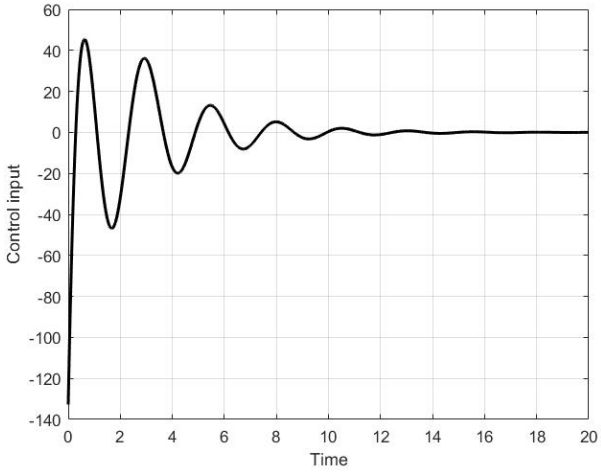

Fig. 8. LQR by Solving DRE by Euler method: Control

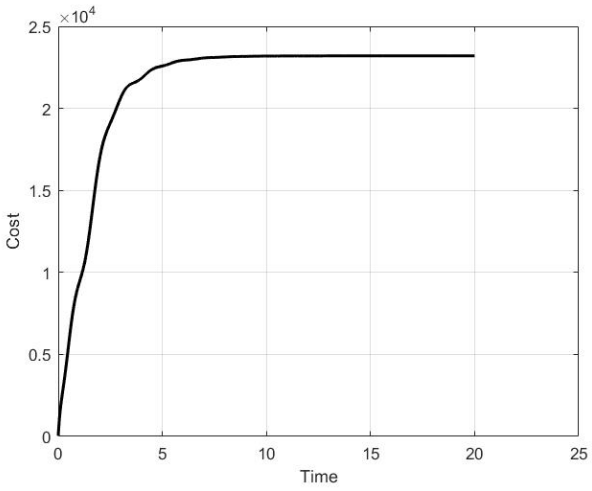

Fig. 9. LQR by Solving DRE by Euler method: Cost Function

for adding these extra inputs and outputs depends on the specific requirements or objectives of the control problem at hand. By extending the system with additional inputs and outputs, we can incorporate additional control signals or measurements that may be necessary to achieve the desired control objectives. And to incorporate the single Riccati equation in the simulation, begin by defining the system dynamics and matrices A, B1, B2, C, and D (Equation 37). Specify the Q (Equation 39) and R weighting matrices for gamma (Equation 41) to balance control effort and state tracking performance. Solve the Riccati equation using the 'icare' function to derive the optimal feedback gain K and update the system dynamics by subtracting the product of B and K from A. Construct the closed-loop system 'sysCl' based on the modified matrices. Lastly, employ MATLAB's plotting functions to visualize the step response and frequency response of the original open-loop system ('sysOl') and the closed-loop system with the optimal controller ('sysCl'). This implementation enables an assessment of the enhanced performance achieved by the optimal controller in terms of step response and frequency response.

We can simulate The double Riccati controller by using system parameters and the model are need to be defined, including the matrices A, B1, B2, C1, and C2 (Eq.37 to Eq.40). and then we need to check Controllability and observability using the PBH test, and the corresponding Gramians are computed. Next, We use LQR controller gains (Eq.47) are obtained by solving two separate Riccati equations (Eq.45-Eq.46). The gains are used to form the full controller gain matrix(Eq.47). When comparing the performance of the LQR single, Riccati, and double Riccati controllers based on step and impulse responses, notable differences emerge. The single Riccati and Riccati controllers demonstrate satisfactory step responses characterized by well-damped behavior (Figure 10). In contrast, the double Riccati controller exhibits improved settling time, reduced overshoot, and enhanced stability. All controllers effectively suppress impulse disturbances. In summary, the double Riccati controller surpasses the single LQR and Riccati controllers in terms of step response characteristics, showcasing superior stability and transient response.

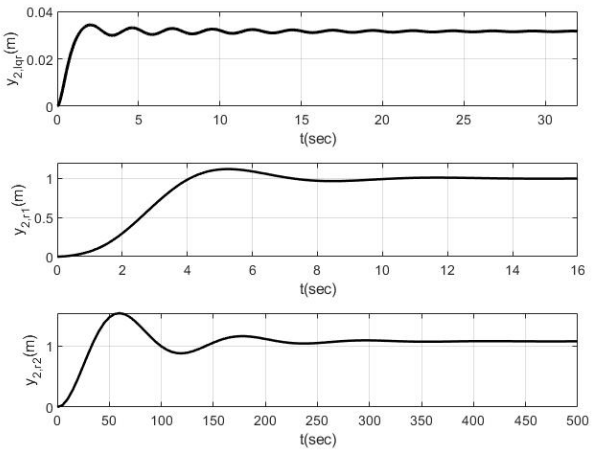

Fig. 10. Response of the system controlled by LQR, H_∞ with One Riccati and H_∞ with Two Riccati Equations with unit step input

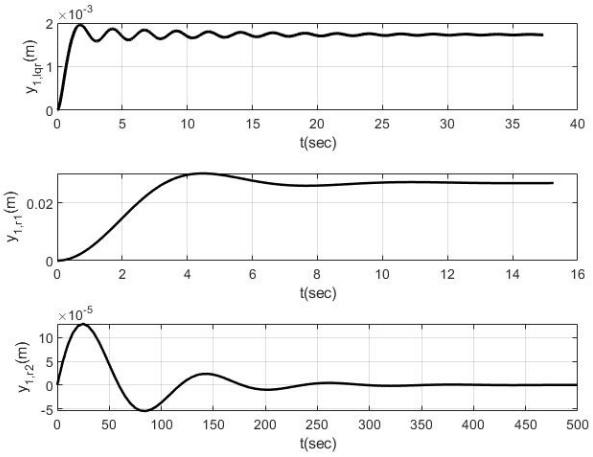

Fig. 11. Response of the system controlled by LQR, H_∞ with One Riccati and H_∞ with Two Riccati Equations with disturbance input

After that. we also made some simulations for HLoop Single Riccati Equation to compare with LQR models in detail. The given program implements a control strategy using the HLoop Single Riccati Equation (HSRE) controller for the system. After applying the controller, the Nyquist plot shows that the system's pole is located at -1 and moves toward infinity. The pole moving toward infinity indicates that the system is stable and well-controlled. The obtained results from running the code indicate that the system has a gain margin of 57.8 dB and a phase margin of 27.2 degrees. These values are derived from the Bode plot, which depicts the system's frequency response. The Bode plot illustrates the system's gain (magnitude) and

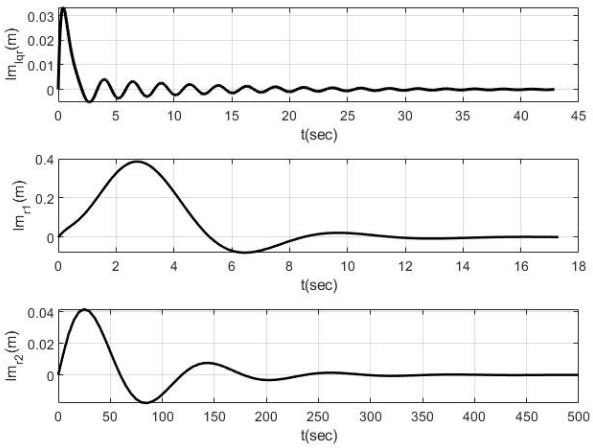

Fig. 12. Response of the system controlled by LQR, H_∞ with One Riccati and H_∞ with Two Riccati Equations with impulse input

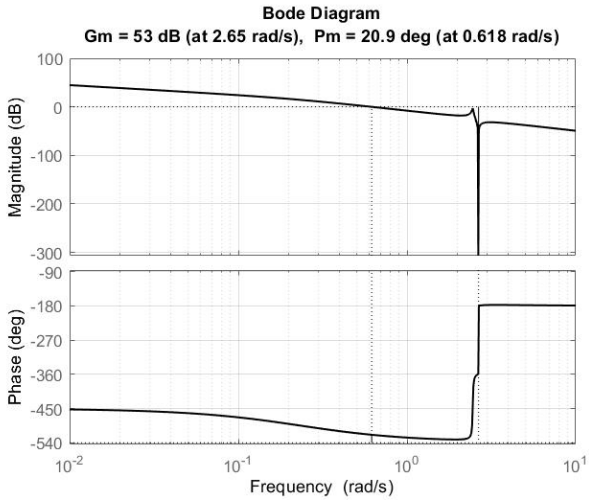

Fig. 13. Bode Plot:LQR

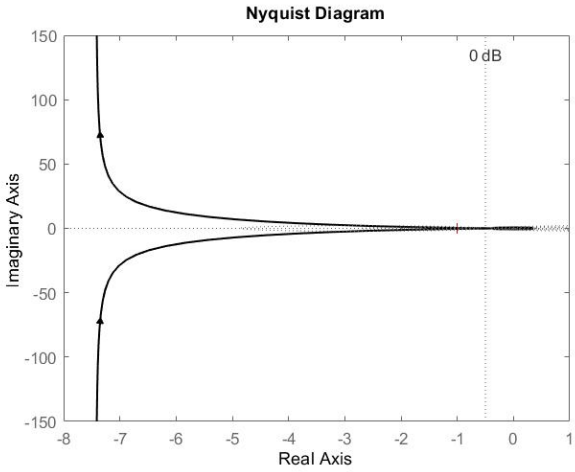

Fig. 14. Nyquist Plot:LQR

phase shift (phase) across different frequencies. Additionally, the Nyquist plot, which shows the system's frequency response in the complex plane, exhibits the presence of a negative pole that approaches infinity. This behavior suggests system stability. A negative pole indicates that the system's transfer function has a stable characteristic, as the pole lies in the left half of the complex plane.

Hence, based on the stability analysis conducted through the Bode and Nyquist plots, we can conclude that the system is stable.

On the other hand, LQR Plot for the Bode diagram displays the gain margin (GM) and phase margin (PM) of the system. In this case, the GM is 53 dB, indicating the system is stable after a few times running so he needs some delay time to be stable position. and Phase Margin is 20.9 degrees and indicates if this system is controllable, denoting the amount of phase shift that the system can tolerate before becoming unstable. A higher PM value signifies a more robust and stable system.

We also made some

In summary, the Nyquist plot and Bode diagram reveal that the HSRE controller effectively stabilizes the system. The Nyquist plot shows the system's stability with the pole at -1, while the Bode plot demonstrates in Figure 15 that the systems have a 57.8dB margin (GM) and a phase margin (PM) of 27.2 degrees, indicating its robustness and stability. These results confirm that the control strategy implemented in the program successfully regulates the system's behavior.

After we got the result from HLoop Single Riccati. we also applying the HLoop Double Riccati Equation controller to the system, the Nyquist diagram shows a pole at -0.6 and -0.2, which moves towards infinity. This indicates that the system is stable, as there are no encirclements of the -1 point in the complex plane. The Bode diagram reveals that the system has a gain margin (GM) of 111 dB, meaning that the system can tolerate and stable. Additionally, the phase margin (PM) is 89.5 degrees, which signifies the amount of phase lag the system can handle before instability occurs. These margins provide insights into the stability and robustness of the controlled system.

The Nyquist plot, depicted in Figure 16, provides insights into the stability and robustness of the controlled system. The plot shows a pole at -1, which moves towards infinity without encircling a point in the complex plane. This confirms the stability of the system under the HLoop Double Riccati Equation controller.

Similarly, the Bode diagram, shown in Figure 17, displays the frequency response of the controlled system. It reveals that the system has a gain margin (GM) is 111dB, indicating the system's ability to tolerate unlimited gain without instability. The phase margin (PM) is 89.5 degrees, representing the amount of phase lag the system can endure before becoming unstable. The Bode plot showcases the robustness of the control design.

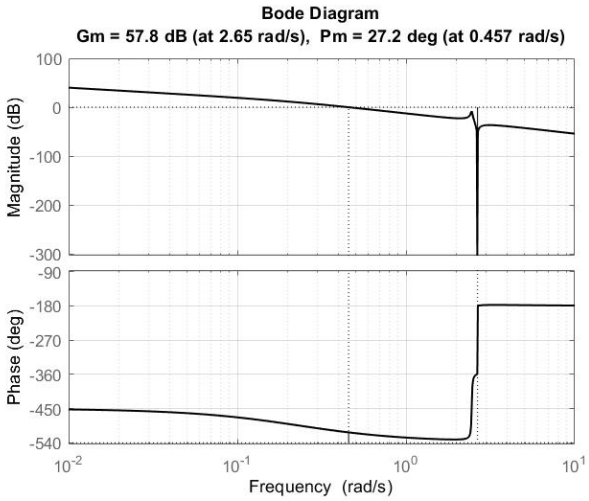

Fig. 15. Bode Plot: H_∞ with One Riccati

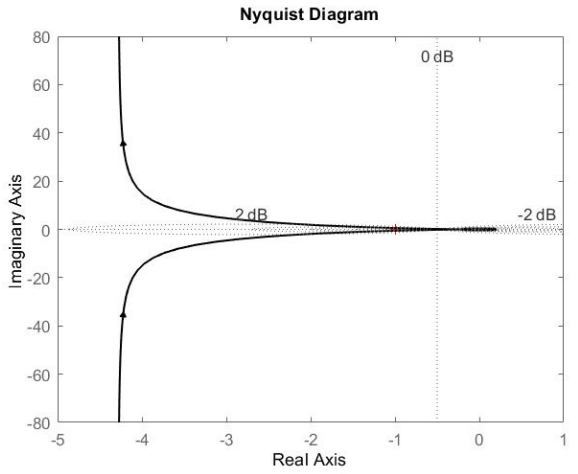

Fig. 16. Nyquist Plot: H_∞ with One Riccati

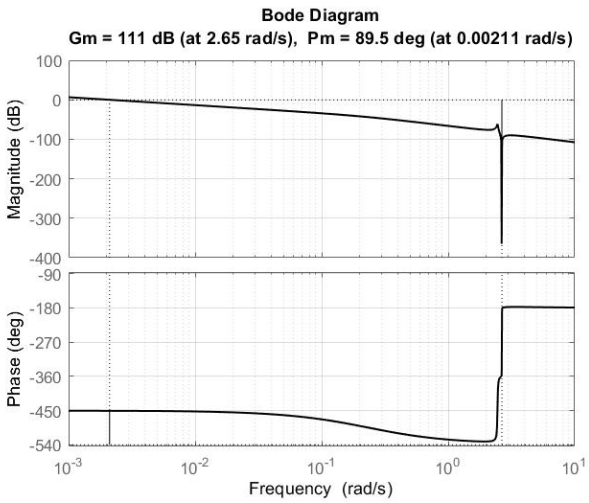

Fig. 17. Bode Plot:H_∞ with Two Riccati Equation

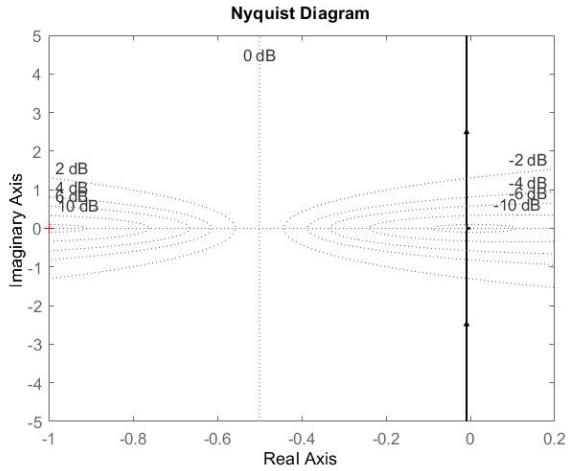

Fig. 18. Nyquist Plot: H_∞ with Two Riccati Equation

C. LFT and Loop Shaping Controller

The loop shaping controller is designed on the basis of a given a open loop which depends on a required cross-over frequency. Let the required cross over frequency is $2.5rad/s^2$. So, the desired loop transfer function $G_d = 2.5/s$. The curve can be given by the figure 19.

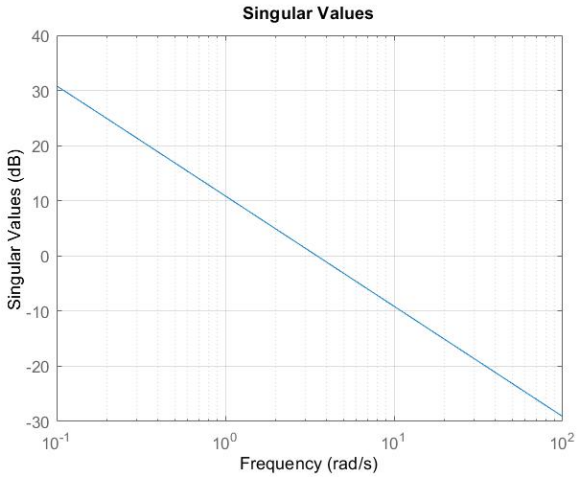

Fig. 19. Desired Loop Transfer Function

Now let add an uncertainty in the IPOC model. Usually sometimes it is difficult to determine exact damping coefficient. Therefore, let us assume the it has 15% uncertainty in there. Therefore the uncertainty can be represented as upper LFT. Using the same augmentation of the system before, the transfer function matrix G can be found. Taking the singular value decomposition of the model, figure 20 depicts that This plant is in bad condition, because it has a gap of about 30 dB between the largest and smallest singular values at $2.5rad/s^2$. The controller can be designed by trading off performance and robustness. For dominance of performance in the design,

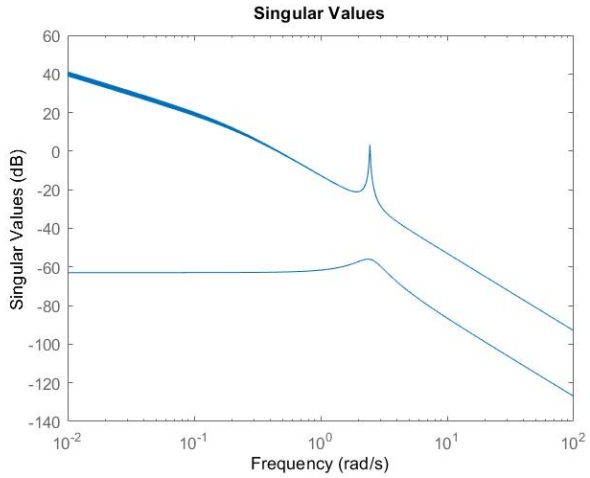

Fig. 20. Singular Value Decomposition of the Model

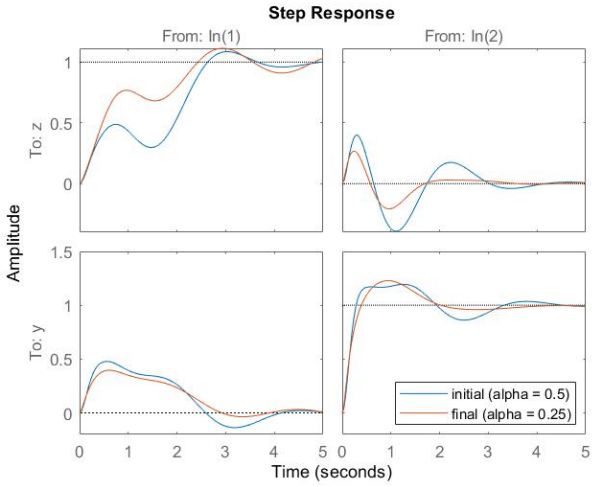

Fig. 22. Step response of the controlled system

at lower frequency, magnitude will be lower than that of highr frequency. For robustness, the at low frequency the magnitude will be always higher than that of high frequency. Therefore two controller with different trade-off criteria can be designed. In one controller, it optimizes performance subject to the robustness being no worse than half the maximum achievable robustness whereas in another controller it slightly prioritize the performance over robustness. This can be expressed with the help of a parameter called α. In these controllers, α values are 0.5 and 0.25 respectively. The figure 21-22 shows that at desired cross over frequency both the controller are close to the desired loop shape although, at lower frequencies the deviation is high enough. From the step response, the implication of trade-off between performance and robustness can be shown. While the margin of first controller is higher, the step response is worse than latter one. Now, Instead of manually augmenting

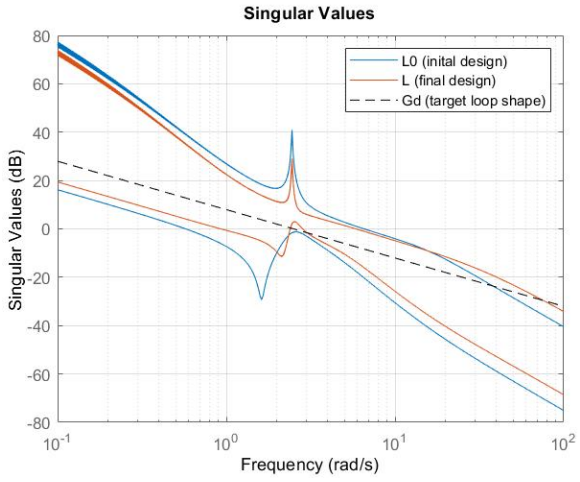

Fig. 21. Loop shaping has been done by the controllers

the system using B_1 and C_1, we can use weighting function to the system to model the system as LFT combining G and K being the lower LFT. the weighting functions $W_1(s)$, $W_2(s)$, and $W_3(s)$ penalizing the error signal, control signal, and output signal, respectively. P can be termed as augmented system transfer matrix. The weighting functions $W_1(s)$ and $W_2(s)$ can be shown in 23 The open loop shape can be shown

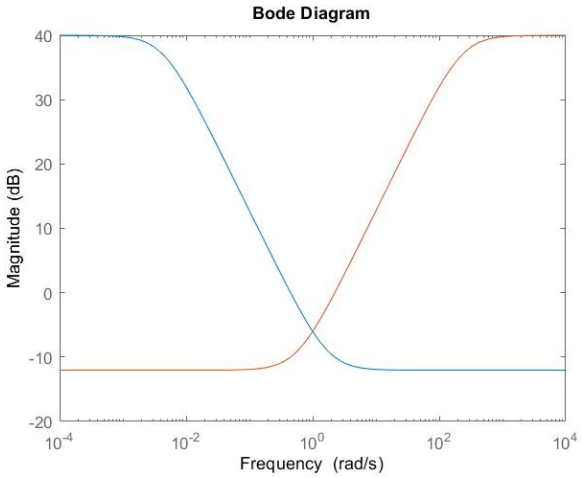

Fig. 23. Weighting Function

by the figure 24 and step response by 25 So, in this section three loop shaping controller has been designed and their $gamma$ are respectively 1.5014, 1.009 1.2153 respectively. Again, disk margin are 0.3792, 0.3769 and 0.3635 respectively.

VI. Conclusion

In conclusion, this paper investigated the control of an inverted pendulum on a cart (IPOC) system, which poses challenges due to its inherent instability and complex dynamics. The study aimed to explore the significance of this problem in control systems research and contribute to the advancement

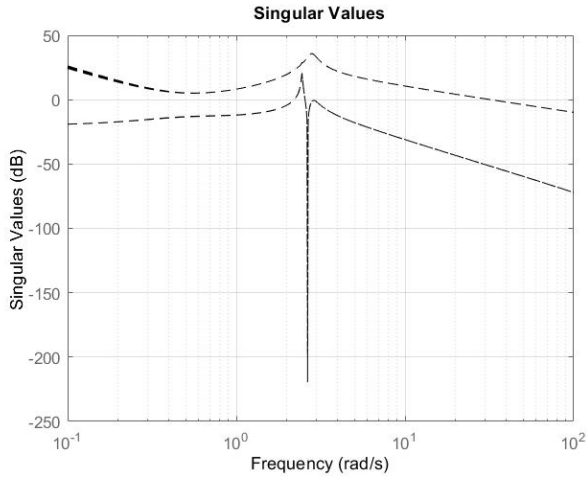

Fig. 24. Loop shaping

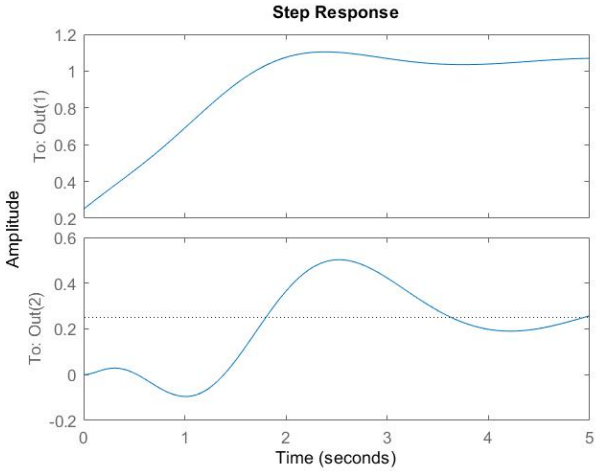

Fig. 25. Step response of the controlled system

of control theory. The simulation results demonstrated the effectiveness of the proposed controllers in stabilizing the IPOC system. The implementation of optimal controllers, based on state feedback using the dynamic programming approach and solving differential Riccati equations, showcased the successful control of the system's state variables, as evidenced by their stability over time. The cost function analysis further validated the optimality of the controllers by minimizing the associated cost. Furthermore, the application of the H-infinity loop controller with single and double Riccati equations showcased its ability to achieve stability and robustness in the IPOC system. The comparison with the LQR controller revealed the advantages of the H-infinity approach, particularly in terms of disturbance rejection and robust performance. Finally three Loop shaping controller is designed based on the trade off criteria. Two weighting functions was designed to augment the model and provide the desired loop shape.

REFERENCES

[1] N. Muskinja and B. Tovornik, "Swinging up and stabilization of a real inverted pendulum," *IEEE transactions on industrial electronics*, vol. 53, no. 2, pp. 631–639, 2006.

[2] E. V. Kumar and J. Jerome, "Robust lqr controller design for stabilizing and trajectory tracking of inverted pendulum," *Procedia Engineering*, vol. 64, pp. 169–178, 2013.

[3] S. Onori, L. Serrao, G. Rizzoni, S. Onori, L. Serrao, and G. Rizzoni, "Pontryagin's minimum principle," *Hybrid Electric Vehicles: Energy Management Strategies*, pp. 51–63, 2016.

[4] Y. Xu, M. Iwase, and K. Furuta, "Time optimal swing-up control of single pendulum," *J. Dyn. Sys., Meas., Control*, vol. 123, no. 3, pp. 518–527, 2001.

[5] M. Weiss and T. Shima, "Linear quadratic optimal control-based missile guidance law with obstacle avoidance," *IEEE Transactions on Aerospace and Electronic Systems*, vol. 55, no. 1, pp. 205–214, 2018.

[6] F. Rinaldi, S. Chiesa, and F. Quagliotti, "Linear quadratic control for quadrotors uavs dynamics and formation flight," *Journal of Intelligent & Robotic Systems*, vol. 70, pp. 203–220, 2013.

[7] V. Van Breusegem, L. Chen, G. Bastin, V. Wertz, V. Werbrouck, and C. de Pierpont, "An industrial application of multivariable linear quadratic control to a cement mill circuit," *IEEE Transactions on Industry Applications*, vol. 32, no. 3, pp. 670–677, 1996.

[8] Y. Tang, Y. Zheng, and N. Li, "Analysis of the optimization landscape of linear quadratic gaussian (lqg) control," in *Learning for Dynamics and Control*, pp. 599–610, PMLR, 2021.

[9] E. F. Camacho and C. B. Alba, *Model predictive control*. Springer science & business media, 2013.

[10] J. Gadewadikar, F. L. Lewis, K. Subbarao, K. Peng, and B. M. Chen, "H-infinity static output-feedback control for rotorcraft," *Journal of Intelligent and Robotic Systems*, vol. 54, pp. 629–646, 2009.

[11] J. Gadewadikar, F. Lewis, K. Subbarao, and B. M. Chen, "Structured h-infinity command and control-loop design for unmanned helicopters," *Journal of guidance, control, and dynamics*, vol. 31, no. 4, pp. 1093–1102, 2008.

[12] S. L. Brunton and J. N. Kutz, *Data-driven science and engineering: Machine learning, dynamical systems, and control*. Cambridge University Press, 2022.